Optical and morphological properties of GaN quantum dots doped with Tm

T. Andreev,[1,*] Y. Hori,[1,2] X. Biquard,[1] E. Monroy,[1] D. Jalabert,[1] A. Farchi,[1] M. Tanaka,[2] O. Oda,[2] Le Si Dang,[3] and B. Daudin[1]

[1]*CEA/CNRS/UJF research group Nanophysique et Semiconducteurs, 17 rue des Martyrs, 38054-Grenoble cedex 9, France*

[2]*NGK Insulators, Ltd., 2-24 Sudacho, Mizuhoku, Nagoya, Japan*

[3]*CEA/CNRS/UJF research group Nanophysique et Semiconducteurs, Laboratoire Spectrométrie Physique (CNRS UMR5588), Université J. Fourier, Boîte Postale 87, 38402 Saint Martin d'Hères, France*

(Received 16 November 2004; published 16 March 2005)

We report on optical and structural properties of wurtzite-phase Tm-doped GaN quantum dots (QDs) embedded in an AlN matrix, grown by plasma-assisted molecular beam epitaxy. The influence of Tm on the size and shape of the QDs is analyzed. The optical properties are studied using cathodoluminescence and photoluminescence. Intra-4*f*-Tm transitions from the $^1D_2$ level show constant temperature behavior from 10 K to room temperature. The internal electric field and strains in the QDs yield a redshift and an additional broadening of the lines. We demonstrate that Tm atoms are partially located in the GaN QDs and partially at the GaN/AlN interface.

DOI: 10.1103/PhysRevB.71.115310 PACS number(s): 78.66.Fd, 68.55.Ln, 85.60.Jb, 68.65.Hb

I. INTRODUCTION

Rare-earth (RE) dopants in wide-band-gap semiconductors like III-nitrides lead to sharp intra-4*f* optical transitions which extend from the infrared to the ultraviolet. Efficient energy transfer from the semiconductor host can take place only if the band-gap energy is higher than the energy level of the rare-earth atoms. After band-to-band excitation of the host semiconductor, the generated free electrons can be captured by a RE-related trap. Next an electron-hole pair can be formed, due to Coulomb interactions. A nonradiative recombination of the pair leads to the excitation of the RE ion, resulting in the observed luminescence. Thus, doping with Eu, Sm, or Pr (red), Er (green and infrared), Tb or Ho (green), and Tm (blue) could provide an alternative solution for full-color light-emitting diodes.[1–8]

The band gap of the (In)GaN host is wide enough to allow RE transitions, in the whole visible range. However, the RE radiative quantum efficiency strongly depends on the carrier-mediated energy transfer process, which has to compete with fast nonradiative recombination channels. To overcome this problem, we propose to dope GaN or InGaN quantum dots (QDs) with RE ions. Then the carrier-mediated energy transfer to the RE should be improved significantly since QDs are particularly efficient carrier trapping centers. Along these lines, optical properties of Eu-doped GaN QDs embedded in an AlN matrix have been studied, showing that confinement in QDs yields an intense and thermally stable red photoluminescence (PL).[9] We also reported that the growth mechanism of GaN nanostructures was drastically affected in the presence of Eu, with strong perturbations of the morphology of the QDs.[10] Based on structural characterizations, namely, extended x-ray absorption fine structure (EXAFS) and Rutherford backscattering spectroscopy (RBS), Eu was found to occupy the Ga site inside the QDs.[9]

In the case of Tm doping, blue electroluminescence from doped GaN films has already been reported.[11–14] However, the PL intensity was found to be much higher in the case of AlN:Tm layers than in the case of GaN:Tm layers. In particular, transitions from the $^1D_2$ level, the most relevant for blue light emission, are not seen in GaN:Tm films.[15–18]

The charge state of the RE ions is directly reflected in the luminescence. In RE^{3+} ions, inner-shell transitions are dominant. The effect of the surrounding host is weak, yielding to sharp luminescence lines, contrary to the much broader lines from RE^{2+} ions, characterized by outer-shell transitions (see, for example, Ref. 19).

The aim of this article is to analyze the effect of Tm doping on the optical and morphological properties of GaN QDs, and to assess the capability of this rare earth for blue light emission at room temperature.

The article is organized as follows. First we show how the morphology of the QDs is affected by the presence of Tm. Next, we discuss optical properties, namely, cathodoluminescence (CL) results on AlN:Tm and GaN:Tm QDs and PL measurements, where the temperature dependence of the transitions can help to assign their origin. We show that the carrier-mediated energy transfer to the $^1D_2$ level is made allowed in doped QDs. Moreover the transitions related to this level are found to be remarkably stable with respect to the temperature. Finally, the issue of the exact location of Tm atoms within the GaN/AlN heterostructure is addressed by discussing EXAFS and RBS results.

II. EXPERIMENT

All experiments were performed using 1-μm-thick AlN pseudosubstrates deposited by metal organic chemical vapor deposition on *c*-sapphire.[20] After a standard chemical degreasing procedure and acid cleaning, they were fixed with indium on a molybdenum sample holder, and introduced into a molecular beam epitaxy chamber equipped with Al, Ga, and Tm effusion cells and a radio-frequency plasma cell to produce active nitrogen. The GaN QDs were grown at a substrate temperature of 720 °C following the Stranski-Krastanow growth mode, i.e., the QDs appear after the depo-

sition of a GaN wetting layer of about two monolayers (MLs).[21,22] The growth conditions were controlled with reflection high-energy electron diffraction, which allows *in situ* monitoring of the QD formation. During the growth of GaN, the Tm shutter was opened in order to dope the material. Next, the QDs were capped by about 12 nm of AlN. This process was repeated several times to achieve superlattices of QD planes. The last layer of QDs was left uncapped to enable morphological analysis by atomic force microscopy (AFM). For morphological studies of the QDs, a series of samples containing 20 planes with various Tm content was grown. A 60-nm-thick AlN:Tm layer and a 200-nm-thick GaN:Tm layer were also grown on an AlN and GaN buffer, respectively, as reference samples for optical experiments.

The Tm mole fraction of the samples was measured by RBS, with a typical uncertainty of ±2%. The Tm content indicated throughout the paper has been calculated by arbitrarily assuming that all Tm atoms are located inside the GaN material. In other words, it is important to notice that RBS provides accurate information on the quantity of Tm in the superlattice, but lacks in the present case the spatial resolution to determine if Tm is incorporated within the GaN QDs or in the AlN spacer.

In order to investigate the exact location of incorporated Tm, EXAFS experiments were performed at beamline FAME (BM30B) at the European Synchrotron Radiation Facility in Grenoble. EXAFS spectra were recorded at the Tm L_{III} edge (8648 eV) in fluorescence mode with a 30-element energy-resolved detector. Experiments were conducted at room temperature, and the 250×250 μm^2 x-ray spot was kept centered during scans by dynamically adjusting the curvature of the second crystal of the Si(220) monochromator and tracking the beam height. Good harmonic rejection and maximal resolution is achieved thanks to two Rh-coated mirrors of adjustable tilt and curvature situated on both sides of the monochromator. The incidence angle of the x-ray beam on the sample's surface was kept constant at around 35°. Energy calibration was made using an Al-capped Tm layer deposited onto a GaN/Al_2O_3 substrate. Baseline extraction was done using the AUTOBK program[23] and data analysis was conducted using the FEFF and FEFFIT package programs.[24] Before both RBS and EXAFS experiments, the samples were chemically cleaned with HCl in order to remove possible segregated Tm atoms from the surface.

Cathodoluminescence was carried out with a FEI Quanta 200 SEM equipped with a Jobin Yvon HR460 monochromator and charge-coupled device camera operating at liquid nitrogen temperature The injected current was 890 pA at a spot size of 0.2 μm. Temperature-dependent PL was measured with the fourth harmonic of a pulsed neodymium-doped yttrium aluminum garnet (Nd:YAG) laser (266 nm), with a pulse width of 0.5 ns, repetition rate of 8 kHz, and average excitation power of 4.5 mW. Complementary measurements of the infrared signal were performed with the 305 nm line of an Ar^+ laser. The spot size of the laser was nonfocused, covering about 2 mm^2 of the sample, in order to minimize the effect of drifts during temperature-dependent measurements. Even in the case of a well-focused spot ($\sim$200 μm) we do not observe significant changes in the spectra due to the high dot densities.

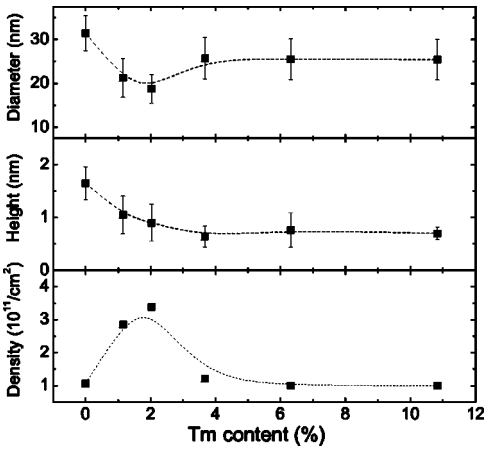

FIG. 1. Diameter, height, and density of QDs measured for samples containing different Tm concentrations. The dashed lines are guides to the eye. The error bars are calculated from Gaussian fits.

III. QUANTUM DOT GROWTH AND MORPHOLOGY

The influence of Tm on the QD nucleation has been studied by AFM. Results are shown in Fig. 1, where the height, diameter, and density of the QDs are displayed as functions of the Tm content. The data are extracted from different AFM images, where about 100 QDs were analyzed. The size distribution of QDs matched well with a Gaussian fit. The distribution of sizes and diameters of the dots is represented by the error bars shown in Fig. 1, which correspond to the standard deviation of the Gaussian fit.

A minimum in diameter and a maximum in density are observed for a Tm content of about 2%. The most significant feature is a decrease of the QD height by a factor of 2 for Tm concentrations higher than 4%. However, these variations in the QD morphology are minimal when compared with those observed in Eu-doped QDs,[10] which indicates a much weaker perturbation of the growth kinetics. It must be also pointed out that Eu, when incorporated in GaN at a concentration higher than 3%, inhibits the nucleation of GaN QDs on AlN.[10] By contrast, in the case of Tm doping, GaN QDs are observed for Tm content higher than 10%. As mentioned in the Sec. II, RBS leads to the determination of a Tm content normalized to the GaN content but does not provide at this stage the location of incorporated Tm. This important issue will be discussed later in Secs. IV and V.

In addition, it is worth noting that both RBS and AFM results indicate a decrease of the amount of GaN deposited for increasing Tm content, reaching 11% for the highest Tm content, as an indication that Ga adatom kinetics is perturbed in presence of Tm.

IV. OPTICAL CHARACTERIZATION

In this section we will analyze the optical properties of AlN:Tm, GaN:Tm, and GaN:Tm QD samples in order to get more insight into the location of Tm^{3+} ions in doped QDs, and to estimate their radiative quantum efficiency with respect to doped thick layers. Both PL and CL measurements

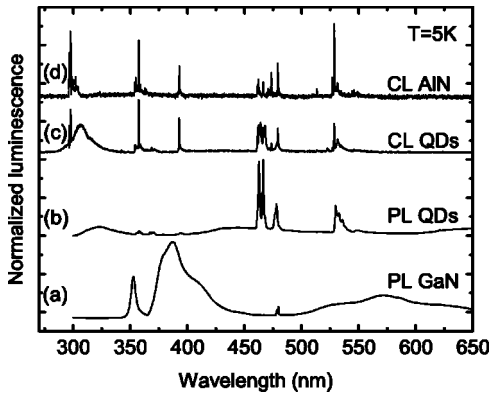

FIG. 2. (a) PL of a GaN:Tm layer; (b) PL of GaN:Tm QDs; (c) CL of GaN:Tm QDs; (d) CL of AlN:Tm at 5 K. In case of the PL spectra, a long-pass filter at 300 nm was used to protect the monochromator from direct laser exposure.

have been performed as a function of the temperature. In PL, only energy levels below 4.6 eV can be excited by the fourth harmonic of the Nd:YAG laser. This limiting value corresponds to about the energy of the wetting layer of GaN/AlN QD samples, but is smaller than the band gap of AlN.[25] Thus PL spectra would mainly display optical transitions from GaN QDs. By contrast, in CL, the generation volume of electrons and holes deeply extends in the sample, typically 500 nm (1 μm) deep in a GaN (AlN) layer for a 10 kV electron beam. As a result, radiative recombinations from both GaN QDs and AlN barriers can be observed, which could provide complementary information about the location of Tm ions.

As shown in Fig. 2(a), the PL spectrum at 5 K of a GaN:Tm thick layer with 2% Tm is dominated by a near-band-edge emission at 355 nm, a strong broadband at 390 nm, and a yellow band at 575 nm. The 390 nm band, not observed in undoped samples, could be related either to some defects induced by Tm doping or to Tm^{2+} ions since divalent rare-earth ions are known to be more sensitive to local crystal field effects than trivalent rare-earth ions. Additional sharp lines at 480 and 805 nm are also observed with considerably weaker intensity [see also Figs. 3(b) and 3(d)]. Using the energy diagram proposed in Ref. 15, they have been identified as originating from the $^1G_4$ and $^3H_4$ levels of Tm^{3+} (see Fig. 4). In this diagram it can be seen that the $^1D_2$ level is nearly resonant with the band gap of GaN. However, no transitions related to this level are observed, in agreement with published literature.[15–18] We will come back to the identification of Tm transition lines at the end of this section.

For Tm-doped QD samples, the situation is markedly different. The 5 K PL spectrum of a GaN QD sample doped with 3% Tm is displayed in Fig. 2(b). First, the spectrum extends further into the ultraviolet (uv), well above the band gap of bulk GaN. Indeed, such a blueshift could be predicted since AFM data in Fig. 1 show that Tm-doped QDs are small, with typical heights less than 1 nm for 3% Tm doping. As a result, in spite of the huge internal electric field in the order of 7 MV/cm in GaN/AlN QDs,[26] carrier confinement effects should be dominant over the quantum confined Stark effect. Therefore we assign the band at 320 nm in Fig. 2(b) to the radiative recombination of electron-hole pairs in QDs. Actually this band peaks at shorter wavelength [i.e., 310 nm, as shown in the CL spectrum in Fig. 2(c)], due to the fact that the uv region of the PL spectrum is severely distorted by the use of a low-band-pass filter at 300 nm to protect the detection system from direct laser exposure. Another striking feature in the PL spectrum is the presence of intense sharp lines related to the $^1I_6$, $^1D_2$, and $^1G_4$ levels in the blue-green region (450–550 nm). These lines, which are not observed for the Tm-doped GaN thick layer [see Fig. 2(a)], are clear evidence of Tm ions in QDs. In fact previous studies of Tm doping in AlGaN alloys have shown that these transition lines can only be detected when the Al concentration is larger than 30%, that is, when the material band gap becomes larger than 4 eV.[17] Indeed this is the case of GaN QDs doped with Tm ions, which suggests that band-gap engineering in semiconductor nanostructures can be used to tune the optical properties of rare-earth ions.

So far we have shown that Tm^{3+} ions are located in doped QDs. However, the carrier-mediated energy transfer to Tm^{3+} ions is not as complete as for Eu-doped QDs, since band-to-band recombination is clearly observed in QDs with 3% Tm [Fig. 2(b)] whereas it is not detectable in QDs with 1.5% Eu.[9] The incomplete energy transfer in Tm-doped QDs cannot be due to a slow energy transfer process, since intense PL of Tm^{3+} is observed at room temperature (see below). This suggests that the Tm concentration in QDs is actually much lower than 3%, implying that most doped Tm^{3+} ions are not in the QDs but in the AlN barrier spacer. It should be noted that our estimate of Tm concentration by RBS is based on the assumption that Tm ions are located only in GaN, which should give an upper limit of Tm concentration in QDs.

More information about Tm^{3+} location is provided by CL measurements, which probe both GaN and AlN parts of the sample. With respect to the PL spectrum in Fig. 2(b), the CL spectrum in Fig. 2(c) of the same doped QD sample indeed exhibits additional lines, next to those of the PL spectrum, but extremely sharp (see details in Fig. 3). These lines are found to coincide with those of the CL spectrum of AlN:Tm [see Fig. 2(d)], which clearly demonstrates that, in doped QDs, Tm^{3+} ions are also present in the AlN barrier layer. The issue of Tm^{3+} location in doped QD samples will be discussed later in more detail with EXAFS analysis.

In Figs. 2 and 3, it can be seen that Tm^{3+} lines in QDs are spectrally broader and redshifted by about 2–3 nm in the blue-green region when compared to AlN:Tm samples. The minimum full width at half maximum (FWHM) is about 1.2 and 0.3 nm in GaN:Tm QDs and AlN:Tm, respectively. This is not so surprising considering the fact that Tm^{3+} in QDs should experience not only strain as large as 1% but also a huge internal electric field of the order of 7 MV/cm. These fields are not uniformly distributed in QDs, which should induce a spectral broadening of Tm^{3+} transition lines. Our FWHM values for AlN:Tm are clearly in the lower limit when compared to results in literature for nitrides doped with rare-earth ions.

Concerning the spectral shift, it is interesting to note that a Stark shift of about 200 kHz/(V/cm) has been reported for the $^4I_{15/2}$-$^4F_{9/2}$ line of Er^{3+} in $YAlO_3$ by application of an external electric field of 200 V/cm.[27] Assuming a similar

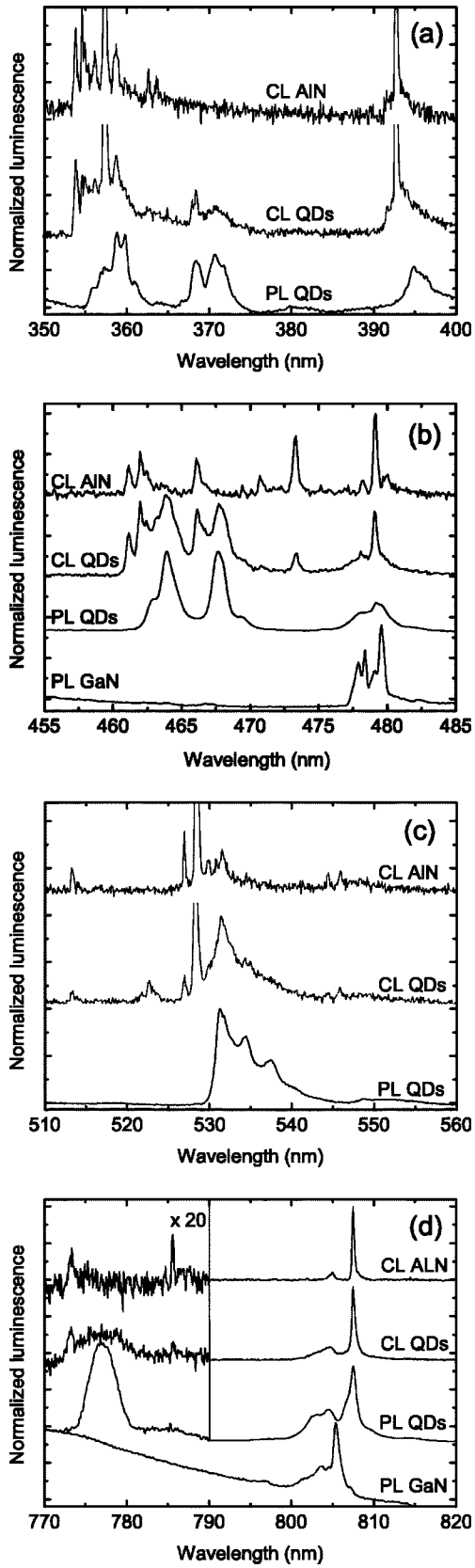

FIG. 3. High-resolution CL and PL spectra of GaN:Tm, GaN:Tm QDs, and AlN:Tm in expended scales (a) from 350 to 400 nm, (b) from 455 to 485 nm, (c) from 510 to 560 nm, and (d) from 770 to 820 nm. The measurements were performed at 5 K.

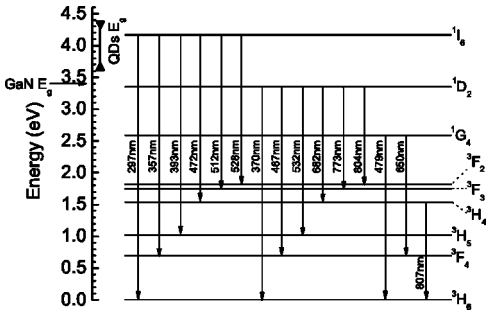

FIG. 4. Energy diagram of Tm^{3+} ions and observed transitions in AlN host. (Compare Figs. 2 and 3.) The energetic position of intra-QD transitions is marked with the arrow at the energy scale. The band gap of GaN at 3.4 eV is also indicated in the figure.

Stark effect, a shift of the order of 0.1 nm would be expected for transition lines in the blue in GaN QDs. Although this rough estimate is smaller by one order of magnitude than measured data, one should keep in mind that electric fields in QDs are on the MV/cm scale, which is 4 orders of magnitude larger than the external applied field. In such a case, nonlinear Stark effects should take place and induce a larger spectral shift.

Finally the key issue of radiative quantum efficiency of doped QDs has been investigated by measuring the temperature dependence of Tm^{3+} PL lines, and results are reported in Figs. 5 and 6. Figures 5(a) and 5(b) show the spectra at 10 and 300 K, where some transition lines become weaker and some others are completely quenched. As displayed in Fig. 5(c), transitions related to the $^1D_2$ level are remarkably stable with respect to the temperature, whereas those related to the $^1I_6$ level are thermally unstable, and those related to the $^3H_4$ and $^1G_4$ levels exhibit an intermediate behavior. It should be noted that, even though the $^3H_4$ and $^1G_4$ levels are deeper in the band gap than the $^1D_2$ level, the carrier-mediated energy transfer is much more efficient to the $^1D_2$ level. This observation strongly supports the existence of an energy transfer trap level close to the $^1D_2$ level, which will be investigated in the future by PL excitation spectroscopy.

In Fig. 6, we compare the temperature dependence of the $^1G_4 \rightarrow {}^3H_6$ Tm^{3+} transition at 480 nm in a GaN layer and in GaN QDs. The superior radiative quantum efficiency of doped QDs is again demonstrated.[9] It can be explained by the high carrier capture cross section of QDs which should enhance any carrier-mediated energy transfer to rare-earth ions. Thus doped QDs appear to be a particularly attractive design structure for light emitters.

The transitions related to GaN QDs and to AlN have been identified by comparing the PL of a GaN:Tm layer, the PL of GaN:Tm QDs, the CL of GaN:Tm QDs, and the CL of AlN:Tm, which have been plotted in expanded scales in Fig. 3 for better clarity.

All transitions identified in this work are summarized in the energy diagram of Fig. 4. The transition wavelengths are those measured in AlN:Tm. Intra-Tm^{3+} transitions in nitrides are assigned to four excited states, namely, the $^1I_6$, $^1D_2$, $^1G_4$, and $^3H_4$ states. However, a final identification of the transitions requires further investigation. This is particularly the case for transitions starting from the $^1I_6$ and $^3P_0$

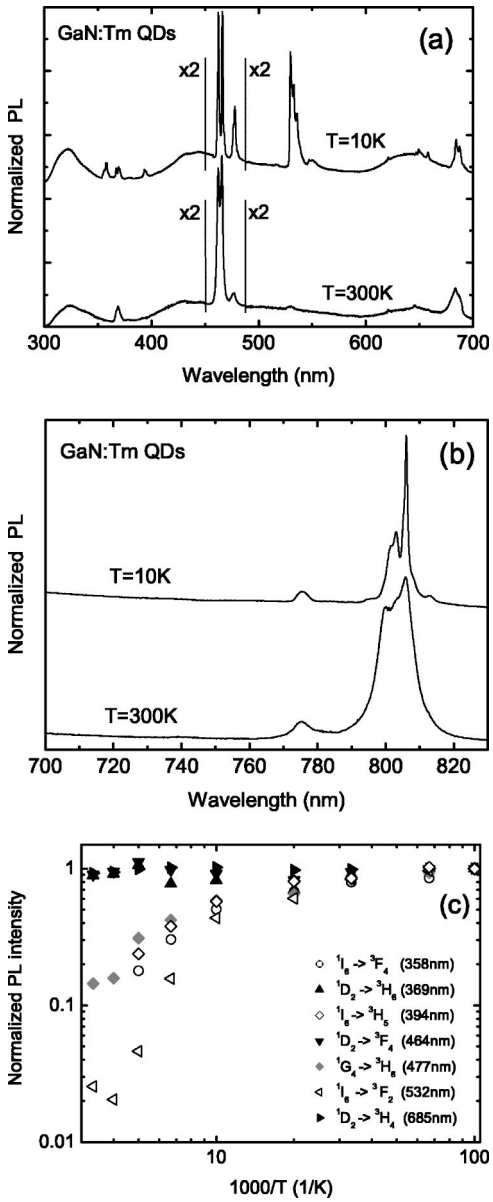

FIG. 5. (a) PL of GaN:Tm QDs measured at 10 and 300 K. The second order of QD signal is observed at around 650 nm. (b) PL spectrum in the infrared region at 10 and 300 K. Excitation source, 305 nm line of an Ar^+ laser. (c) Temperature dependence of the PL intensity for GaN:Tm QDs. The integrated intensity was measured corresponding to each transition. For temperatures higher than 200 K the emission from the $^1I_6 \rightarrow {}^3H_5$ and $^1I_6 \rightarrow {}^3F_4$ transitions was under the detection limit. Excitation source, 266 nm from a Nd:YAG laser.

levels.[15,28,29] It is worth noting that, for some of the energy levels, a splitting has been observed, which can be explained by considering spin-orbit interaction or crystal field splitting, which is discussed in Ref. 30, and was found for Tm^{3+} in single-crystalline materials. (See, for instance, Refs. 27 and 31.)

As mentioned above, the temperature dependence of transition lines is a good indication of their origins. For example, in doped QDs, transitions related to the $^1D_2$ level are remarkably stable with respect to the temperature, whereas those

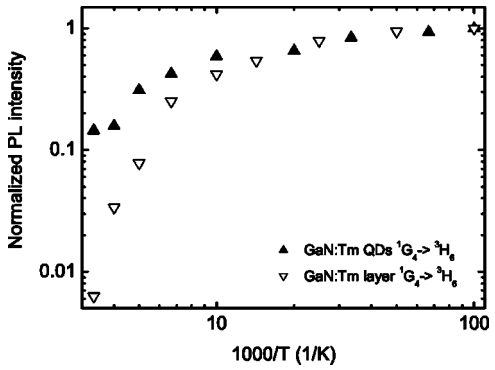

FIG. 6. Temperature dependence of the PL for the $^1G_4 \rightarrow {}^3H_6$ transition in a GaN:Tm layer and in GaN:Tm QDs.

related to the $^1I_6$ level are strongly quenched at room temperature [see Fig. 5(a)]. On the other hand, at low temperature, the $^1I_6$ transitions are dominant in the CL spectra of AlN:Tm and doped QDs, but much weaker in the PL spectrum of doped QDs. This illustrates the complexity of the carrier-mediated energy transfer. In CL experiments, carriers can be excited in AlN, which could favor their capture into a Tm-related trap for energy transfer to the $^1I_6$ level of Tm ions in AlN. In PL experiments, carriers are excited only in QDs and our results suggest that the energy transfer takes place

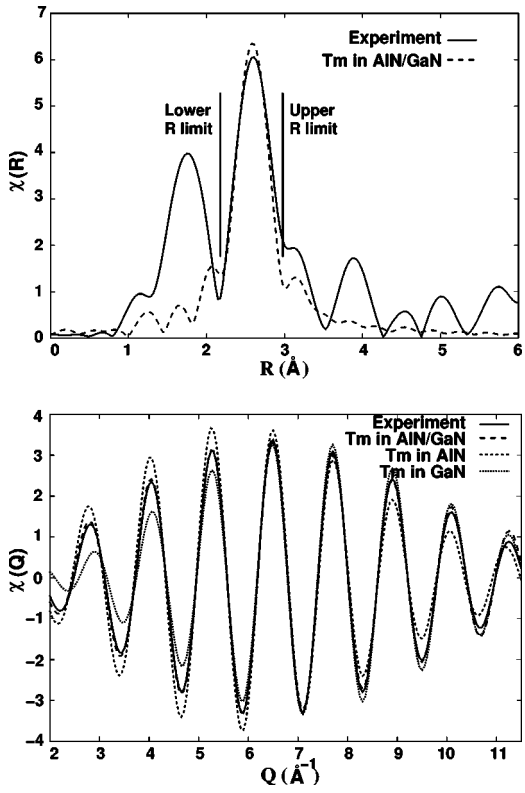

FIG. 7. Comparison between experimental (solid line) and calculated EXAFS spectra in *R* space (top figure, not phase corrected) and *q* space (bottom figure, *R* ranging from 2.1 to 2.9). Long dashed line represents simulation assuming Tm incorporation inside AlN/GaN, dashed line assuming Tm incorporation inside AlN, and short dashed line incorporation inside GaN QDs.

TABLE I. Best EXAFS fitting parameters for a sample consisting of 3% Tm-doped GaN QDs embedded in AlN. Fitting was achieved assuming an amplitude reduction factor $S_0^2=0.8$ and a coordination number of 12. Bond length distortion makes reference to the undistorted wurtzite structure of GaN or AlN, in which the Al-Al distance is 3.092 Å and the Ga-Ga distance is 3.185 Å.

Second-nearest-neighbor shell	Tm in GaN	Tm in AlN	Tm in (GaN, AlN)	
			GaN	AlN
Proportion (%)			25±4	75±4
Bond length distortion (%)	−1.6±0.8	0.0±0.7	−1.7±0.6	+1.8±0.8
Debye-Waller factor (10^{-3} Å^2)	13±1	10±1	5±4	
Energy shift (eV)	−21±4	−6±2	−2±3	
r factor (quality) of fit (%)	3.4	3.9	0.2	

via the $^1D_2$ level rather than the $^1I_6$ level of Tm in QDs.

As a whole, from the comparison of optical data obtained by the two experimental methods, namely, PL and CL, we can conclude that Tm is incorporated inside the GaN QDs and also in the AlN spacer. Specific QD-related intra-Tm transitions also exist, which was demonstrated by the comparison of the AlN:Tm layer and the GaN:Tm QDs in CL. This was confirmed by PL, which revealed that Tm transitions related to QDs show constant PL as a function of temperature.

V. STRUCTURAL CHARACTERIZATION

To confirm the conclusions of the optical studies and to overcome the lack of spatial resolution of the RBS, EXAFS experiments have been performed in order to identify the chemical environment of Tm atoms. Recorded spectra show a single contribution in the L_{III} edge at 8648.6 eV, attributed to Tm^{3+}, and EXAFS oscillations were extracted relative to this edge. EXAFS results obtained on the 3% doped QD sample are presented in Fig. 7.

These results are consistent with Tm located in a Ga or Al substitutional site, showing four nitrogen atoms as the first neighbors. To determine whether Tm has been incorporated within GaN or AlN, we have to assess the chemical nature of the second-nearest-neighbor shell of Tm: 12 Ga for Tm inside GaN QDs and 12 Al inside AlN matrix. The large mass discrepancy between Al(13) and Ga(31) should make it easy to distinguish between Al and Ga as the backscatterer. The pseudoradial distribution in *R* (upper part in Fig. 7, not phase corrected) was obtained by taking the norm of the Fourier transform of $k^3\chi(k)$ (not shown), with *k* ranging from 2.2 to 11.05 Å^{-1}.

The pseudoradial distribution in *R* presents numerous consecutive peaks corresponding to the various shells around Tm inside GaN or AlN. The first-nearest-neighbor shell consisting of four nitrogen atoms (lightest element) gives rise to the first peak at 1.7 Å, while the second-nearest-neighbor shell consisting of 12 heavier elements (Al or Ga) gives rise to the most important peak at 2.6 Å. Therefore, EXAFS analysis was conducted on this second peak by using the Fourier back transform (lower part in Fig. 7), with *R* ranging from 2.1 to 2.9 Å. Table I shows the best EXAFS fitting parameters for the studied sample. The *r* factor of the fit is too high when assuming Tm incorporated either within GaN QDs or within the AlN matrix. Therefore, the Tm local environment should consist of a combination of both GaN and AlN, and we have to determine the relative proportions of GaN and AlN. The straightforward solution would be to adjust our data using independent fit parameters for GaN and AlN, plus a proportionality factor. However, this will lead to using more parameters than degrees of freedom. Therefore, we choose to use independent parameters only for the bond length since EXAFS is particularly sensitive to distances. The optimum fit is then obtained using a proportion of 1/4 of GaN and 3/4 of AlN. Moreover, the small energy shift found is compatible with the small energy shift of 0.6 eV found between the reference metallic Tm and the studied sample.

It is worth noting that fit parameters naturally depend on the chosen value for S_0^2. Using for the range of variation of S_0^2 the common interval $[0.7:0.9]$, one obtains the best-fit pa-

TABLE II. Influence of the reduction factor S_0^2 on the best EXAFS fitting parameters, assuming a coordination number of 12 for the second shell.

Tm in (GaN, AlN)	$S_0^2=0.7$		$S_0^2=0.8$		$S_0^2=0.9$	
	GaN	AlN	GaN	AlN	GaN	AlN
Proportion (%)	22±6	88±6	25±4	75±4	29±4	71±4
Bond length distortion (%)	−2.4±0.5	+1.4±0.7	−1.7±0.6	+1.8±0.8	−1.3±0.6	2.1±1.0
Debye-Waller factor (10^{-3} Å^2)	3±4		5±4		6±4	
Energy shift (eV)	−3±2		−2±3		−3±3	
r factor (quality) of fit (%)	0.15		0.2		0.3	

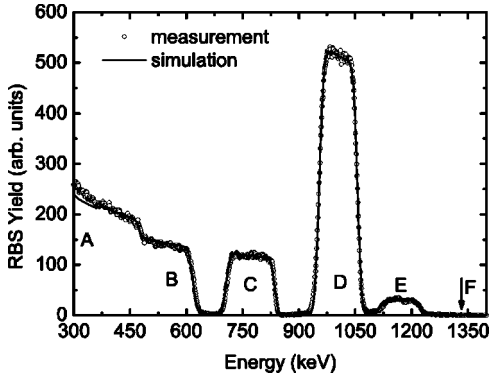

FIG. 8. RBS spectrum of a sample containing a 104 nm GaN:Tm layer with 180-nm-thick AlN:Tm on top. Acceleration voltage of the He ions, 1.5 MeV. Tm content inside GaN, 1.2%. The letters are used to label the positions of elements: *A* is N in AlN, GaN:Tm, and AlN:Tm; *B* is Al in AlN of the substrate; *C* is Al in AlN:Tm; *D* is Ga in GaN:Tm; *E* is Tm in GaN:Tm. The arrow at the letter *F* indicates the calculated position of Tm in AlN.

rameters presented in Table II. On the whole range $[0.7:0.9]$, we obtained a good *r* factor of the fit, the corresponding Fourier back transform spectra (not shown) being almost indistinguishable one from another, and the intervals of variation for the fit parameter are all consistent. Therefore, fit parameters obtained for $S_0^2=0.8$ may be considered as reliable. In summary, EXAFS results could indicate at first view that part of the Tm atoms diffuse into the AlN lattice.

To further assess the diffusion of Tm into AlN, we have analyzed the incorporation rate of Tm in GaN and AlN by RBS. For this purpose, a sample consisting of a 104-nm-thick GaN:Tm layer capped by a 180-nm-thick AlN:Tm film was grown on an AlN template. During the growth of both layers the Tm flux remained constant. Figure 8 shows a RBS spectrum corresponding to the sample described above. Quantitative analysis demonstrated that Tm concentration in the GaN layer was 1.2%, contrary to the AlN layer where incorporated Tm is below the RBS detection limit of our system ($\sim$0.025%), as evidence that Tm incorporation in AlN is much lower than its incorporation in GaN, for a fixed Tm flux. Then, the atomic distribution of 1/4 Ga second neighbors and 3/4 Al second neighbors obtained by EXAFS can be interpreted by assuming that the Tm atoms are mostly located at the AlN/GaN interface in AlN and it does not result from a random incorporation in both GaN and AlN. This is supported by the fact that the Tm-Ga distance is always shorter as compared to undisturbed wurtzite in our EXAFS best fits, while the Tm-Al bond distance is always longer: both distances are found equal to 3.14 ± 0.02 Å. Nevertheless, EXAFS results could be alternatively interpreted by assuming that Tm is mostly incorporated in a $Ga_{0.25}Al_{0.75}N$ alloy. Such an alloy could result from capping of GaN QDs with AlN. At 720 °C, which was the standard growth temperature for the work presented here, capping effects are negligible,[32] although intermixing in the range of one monolayer cannot be totally discarded.[33]

The demonstration that most Tm is segregated at the interface between AlN and GaN QDs provides insights into the physical meaning of large Tm content in GaN QDs extracted from RBS experiments. Although contents as large as 10%, normalized to GaN content are meaningless, the evidence for Tm segregation makes them understandable: the nominal GaN coverage rate being 5 ML, the segregation of a full monolayer of Tm at the GaN/AlN interface would lead to a Tm content of about 20%, normalized to GaN content, in qualitative agreement with EXAFS and RBS results.

VI. CONCLUSIONS

In summary we have studied morphological properties of GaN QDs doped with Tm and found that the nucleation kinetics is not significantly perturbed by the presence of Tm. EXAFS experiments combined with RBS indicate that Tm is located at the interface of the QDs, mostly inside the surrounding AlN layer. These structural results are consistent with CL results which have been interpreted by assuming that Tm is located inside QDs but also in the surrounding AlN spacer. Transitions that are QD related show constant temperature behavior, a shift, and broader linewidths, likely resulting from the presence of a large internal electric field.

ACKNOWLEDGMENTS

We acknowledge Marlène Terrier, Yann Genuist, Gilbert Demoment, and Yoann Curé for their technical assistance, and Fabrice Donatini for the development of the cathodoluminescence experiment.

*Corresponding author: Thomas Andreev. Electronic address: andreev@drfmc.ceng.cea.fr

[1] D. S. Lee and A. J. Steckl, Appl. Phys. Lett. **81**, 2331 (2002).
[2] S. Morishima, T. Maruyama, M. Tanaka, Y. Masumoto, and K. Akimoto, Phys. Status Solidi A **176**, 113 (1999).
[3] S. Morishima, T. Maruyama, and K. Akimoto, J. Cryst. Growth **209**, 625 (1999).
[4] J. Steckl, M. Garter, D. S. Lee, J. Heikenfeld, and R. Birkhahn, Appl. Phys. Lett. **75**, 2184 (1999).
[5] H. J. Lozykowski, M. Jadwisienczak, and I. Brown, Appl. Phys. Lett. **74**, 1129 (1999).
[6] Z. Li, H. Bang, G. Piao, J. Sawahata, and K. Akimoto, J. Cryst. Growth **240**, 382 (2002).
[7] K. Hara, N. Ohtake, and K. Ishii, Phys. Status Solidi B **216**, 625 (1999).
[8] H. Bang, S. Morishima, Z. Li, K. Akimoto, M. Nomura, and E. Yagi, J. Cryst. Growth **237–239**, 1027 (2002).
[9] Y. Hori, X. Biquard, E. Monroy, D. Jalabert, F. Enjalbert, Le Si Dang, M. Tanaka, O. Oda, and B. Daudin, Appl. Phys. Lett. **84**, 206 (2004).
[10] Y. Hori, D. Jalabert, T. Andreev, E. Monroy, M. Tanaka, O. Oda, and B. Daudin, Appl. Phys. Lett. **84**, 2247 (2004).

[11] D. S. Lee and A. J. Steckl, Appl. Phys. Lett. **83**, 2094 (2003).
[12] Y. Q. Wang and A. J. Steckl, Appl. Phys. Lett. **82**, 502 (2003).
[13] J. H. Kim, M. R. Davidson, and P. H. Holloway, Appl. Phys. Lett. **83**, 4746 (2003).
[14] Y. Q. Wang and A. J. Steckl, Appl. Phys. Lett. **82**, 502 (2003).
[15] U. Hömmerich, Ei Ei Nyein, D. S. Lee, A. J. Steckl, and J. M. Zavada, Appl. Phys. Lett. **83**, 4556 (2003).
[16] U. Hömmerich, Ei Ei Nyein, D. S. Lee, J. Heikenfeld, A. J. Steckl, and J. M. Zavada, Mater. Sci. Eng., B **105**, 91 (2003).
[17] D. S. Lee and A. J. Steckl, Appl. Phys. Lett. **83**, 2094 (2003).
[18] H. J. Lozykowski, M. Jadwisienczak, and I. Brown, Appl. Phys. Lett. **74**, 1129 (1999).
[19] J. F. Owen, P. B. Dorain, and T. Kobayasi, J. Appl. Phys. **52**, 1216 (1981).
[20] T. Shibata, K. Asai, T. Nagai, S. Sumiya, M. Tanaka, O. Oda, H. Miyake, and K. Hiramatsu, in *GaN and Related Alloys–2001*, edited by J. E. Northrup, J. Neugebauer, D. C. Look, S. F. Chichibu, and H. Riechert, MRS Symposia Proceedings No. 693 (Materials Research Society, Pittsburgh, 2002).
[21] F. Widmann, B. Daudin, G. Feuillet, Y. Samson, J. L. Rouvière, and N. Pelekanos, J. Appl. Phys. **83**, 7618 (1998).
[22] I. N. Stranski and L. Krastanow, Sitzungsber. Akad. Wiss. Wien, Math.-Naturwiss. Kl., Abt. 2B **146**, 797 (1937).
[23] M. Newville, P. Livins, Y. Yacoby, J. J. Rehr, and E. A. Stern, Phys. Rev. B **47**, 14 126 (1993).
[24] M. Newville, B. Ravel, D. Haskel, J. J. Rehr, E. A. Stern, and Y. Yacoby, Physica B **208–209**, 154 (1995).
[25] C. Adelmann, E. Sarigiannidou, D. Jalabert, Y. Hori, J.-L. Rouvière, B. Daudin, S. Fanget, C. Bru-Chevallier, T. Shibata, and M. Tanaka, Appl. Phys. Lett. **82**, 4154 (2003).
[26] J. Simon, N. T. Pelekanos, C. Adelmann, E. Martinez-Guerrero, R. André, B. Daudin, Le Si Dang, and H. Mariette, Phys. Rev. B **68**, 035312 (2003).
[27] Y. P. Wang and R. S. Meltzer, Phys. Rev. B **45**, 10 119 (1992).
[28] G. H. Dieke, *Spectra and Energy Levels of Rare Earth Ions in Crystals* (Wiley, New York, 1968).
[29] M. D. Seltzer, J. B. Gruber, M. E. Hills, G. J. Quarles, and C. A. Morrison, J. Appl. Phys. **74**, 2821 (1993).
[30] A. J. Kenyon, Prog. Quantum Electron. **26**, 225 (2002).
[31] M. D. Seltzer, J. B. Gruber, M. E. Hills, G. Quarles, and C. A. Morrison, J. Appl. Phys. **74**, 2821 (1993).
[32] E. Sarigiannidou, E. Monroy, P. Bayle-Guillemaud, N. Gogneau, B. Daudin, and J. L. Rouvière, Superlattices Microstruct. (to be published).
[33] N. Gogneau, D. Jalabert, E. Monroy, E. Sarigiannidou, J. L. Rouvière, T. Shibata, M. Tanaka, J. M. Gerard, and B. Daudin, J. Appl. Phys. **96**, 1104 (2004).